Published in final edited form as:
Science. 2013 April 12; 340(6129): 207–211. doi:10.1126/science.1235214.

Persistent LCMV infection is controlled by blockade of type 1 interferon signaling

John R. Teijaro[1,**], **Cherie Ng**[1,**], **Andrew M. Lee**[1], **Brian M. Sullivan**[1], **Kathleen C.F. Sheehan**[2], **Megan Welch**, **Robert D. Schreiber**[2], **Juan Carlos de la Torre**[1], and **Michael B. A. Oldstone**[1,*]

[1]Department of Immunology and Microbial Science, The Scripps Research Institute, La Jolla, CA 92037

[2]Department of Pathology and Immunology, Washington University School of Medicine, St. Louis, MI 63110

Abstract

During persistent viral infections, chronic immune activation, negative immune regulator expression, an elevated interferon signature and lymphoid tissue destruction correlate with disease progression. Here, we demonstrate that blockade of type 1 interferon (IFN-I) signaling using a type 1 interferon receptor neutralizing antibody reduced immune system activation, decreased expression of negative immune regulatory molecules and restored lymphoid architecture in mice persistently infected with lymphocytic choriomeningitis virus (LCMV). IFN-I blockade both prior to and following establishment of persistent virus infection resulted in enhanced virus clearance and was CD4 T-cell-dependent. Hence, we demonstrate a direct causal link between IFN-I signaling, immune activation, negative immune regulator expression, lymphoid tissue disorganization and virus persistence. Our results suggest therapies that target IFN-I may help control persistent virus infections.

Persistent viral infections such as HIV, HBV and HCV represent significant global health problems. Persistent viruses take advantage of negative immune regulatory molecules to suppress antiviral CD4 and CD8 T-cell responses (1, 2), resulting in T-cell exhaustion (3, 4), facilitating virus persistence. Hyper-immune activation is also observed following persistent virus infection and is characterized by prolonged activation of T-cells, B cells and NK cells, elevated pro-inflammatory mediators, and a sustained interferon signature (5–7). Type 1 interferon (IFN-I) signaling is upstream of hundreds of inflammatory genes, suggesting that IFN-I may be responsible for generating the hyper-activated immune environment during virus persistence. We investigated the role of IFN-I in regulating immune activation, immune suppression and virus control following persistent virus infection in mice.

To elucidate the role of IFN-I in virus persistence, we utilized LCMV. In adult mice, the Armstrong (Arm) strain causes an acute infection that is cleared 8 days post-infection (dpi) due to robust antiviral CD8 T-cell responses. In contrast to the Arm strain, the clone-13 (Cl13) strain causes a systemic viral infection lasting over 90 days (8–13). Cl13-infected mice had significantly elevated IFN-I in the serum compared to Arm-infected counterparts at 18 and 24 hours post-infection (hpi) (Fig. 1A&B). Using IFN-β-YFP reporter mice (14), we detected YFP expression in plasmacytoid dendritic cells (pDCs) at 18-hours post-Cl13

*Corresponding author: Michael B.A. Oldstone, IMM-6, TSRI, 10550 N. Torrey Pines Rd, La Jolla, CA 92037. Phone: (858) 784-8054; Fax: (858) 784-9981, mbaobo@scripps.edu; To whom reprint requests should be sent.
**These authors contributed equally to this work

infection, with minimal YFP expression in pDCs during Arm infection (Fig. S1A). IFN-β-YFP expression was not observed in other splenocytes (Fig. S1B), suggesting that Cl13 infection induces IFN-β production in pDCs. pDCs are reported to be an early target of Cl13 infection (13, 15). To address whether Cl13 preferentially infected pDCs, we utilized non-replicating Arm or Cl13 viruses, in which their glycoprotein's (GP) were replaced with a GFP marker (denoted ΔGP-Cl13 or ΔGP-Arm). As expected, pDCs exhibited a 2- to 2.5-fold increase in GFP expression upon infection with ΔGP-Cl13 compared to ΔGP-Arm (Fig. 1C). Consistent with IFN-I signaling being upstream of inflammatory gene expression, we observed elevated expression of multiple pro-inflammatory cytokines and chemokines 18 hours post-Cl13 infection vs. Arm infection (Fig. S1C). To determine if elevated pro-inflammatory cytokines and chemokines in Cl13 infection were due to IFN-I signaling we treated mice with an anti-Interferon alpha-beta receptor 1 (IFNAR1) antibody prior to infection and measured cytokine and chemokine levels in the serum 18, 24 and 48 hpi (16). Blockade of IFN-I signaling significantly blunted production of multiple pro-inflammatory cytokines and chemokines following Cl13 infection at 18, 24 and 48 hpi (Fig. S1C–E).

We asked whether IFN-I signaling contributes to the Cl13-induced immunosuppressive state. IFN-I signaling blockade resulted in significant suppression of IL-10 production 1 and 5 dpi (Fig. 2A). We also detected significant suppression of PD-L1 on both $CD8\alpha^+$ and $CD8\alpha^-$ DCs 1 dpi (Fig. 2B), which was retained 5 and 9 dpi in $CD8\alpha^-$ DCs but not in $CD8\alpha^+$ DCs (Fig. 2C & D). Together, these results demonstrate that IFN-I signaling inhibits negative regulatory molecule expression. Because DCs are primary targets of Cl13 infection and DC infection is crucial for virus persistence (8,17,18), we asked whether blockade of IFN-I signaling altered the DC compartment. IFN-I blockade increased virus nucleoprotein (NP) expression in DCs and macrophages 5 dpi (Fig. S2C). Blockade of IFN-I signaling significantly increased both the frequency and number of $CD8\alpha^-$ and $CD8\alpha^+$ DCs and macrophages (Fig. S2A). Moreover, we observed a significant increase in DCs with an immune-stimulatory phenotype following blockade of IFN-I signaling (Fig. S2B).

The regulation of IL-10 and PD-L1 expression by IFN-I led us to investigate how IFN-I affects the immune environment during persistent virus infection. IFN-I blockade prior to Cl13 infection resulted in increased splenocyte numbers in anti-IFNAR1 compared to control treated mice 9 dpi (Fig. S3A). This correlated with significant increases in B-cells, CD4 and CD8 T-cells, NK cells, DCs and macrophages (Fig. S3B & C). Although IFN-I blockade resulted in early inhibition of multiple pro-inflammatory cytokines and chemokines and negative immune regulatory molecules following Cl13 infection (Fig. 2 and S1C–E), we detected increases in Interferon-gamma (IFN-γ) production 24 hpi (Fig. S2D) and similar levels of pro-inflammatory cytokines and chemokines 5dpi (Fig. S3D).

Lymphoid architecture is integral to induction and maintenance of immune responses (19–23) . Cl13 infection resulted in severe lymphoid disorganization (23) with indistinguishable marginal zones and follicular structures and scattered B and T-cell zones 9dpi (Fig. 2E), which was more apparent 14dpi (Fig. 2F). IFN-I blockade preserved splenic architecture, with white pulp, follicle margins and T and B cells zones appearing similar to naïve spleens (Fig. 2E, middle and bottom). Fibroblastic reticular cell staining (ER-TR7; Fig 2E, middle row) highlighted preservation of splenic organization and architecture following IFN-I blockade. These data demonstrate that IFN-I signaling contributes to splenic architecture disorganization during Cl13 infection.

We next asked whether blockade of IFN-I signaling altered control of Cl13. IFN-I blockade resulted in increased percentages of lymphocytes expressing LCMV viral antigen 24 hpi (Fig. S2 C&D) and significantly higher Cl13 titers in the serum 10 dpi (Fig. 3A), suggesting anti-IFNAR1 antibody treatment blocked early antiviral effects of IFN-I. Surprisingly, by 30

dpi, we observed significant reductions in Cl13 titers following IFN-I blockade (>1.5-logs) compared to isotype control treated mice (Fig. 3A). By 40 dpi, IFN-I blockade resulted in significant reductions of viral titers in both serum and tissues (Fig. 3B). By 50 dpi, virus was undetectable in the serum following IFN-I blockade while control mice retained >3 logs of virus (Fig. S4A), demonstrating that IFN-I blockade hastens clearance of Cl13 infection.

IFN-I transcripts are detectable in DCs several weeks following Cl13 infection (24). We postulated that blocking IFN-I signaling during an established Cl13 infection would result in faster viral clearance. Following an initial spike in viral titers 20 dpi, we observed >1-log reduction in serum viral titers in anti-IFNAR1 compared to isotype-treated mice by 40 dpi (Fig. S4B). By 50 dpi, 75% of the anti-IFNAR1 treated mice had undetectable levels of virus while 75% of control animals maintained >3 logs of virus (Fig. 3D). Analysis of virus in liver and lung 50 dpi revealed reductions in viral titers in both tissues following IFN-I blockade (Fig. 3D). These results demonstrate therapeutic potential of IFN-I signaling blockade.

We asked whether enhanced virus clearance following IFN-I blockade could be duplicated following Arm infection. IFN-I blockade during Arm infection resulted in significantly elevated viral titers in the serum compared to control mice (Fig. S5A). Anti-IFNAR1 treated animals maintained >3 logs of virus in serum 20 dpi (Fig. S5B). Moreover, following IFN-I blockade viral titers were detectable in lung, kidney and brain 30 dpi, a time when virus was undetectable in tissues of control mice (Fig. S5C). The inability to clear Arm correlated with reduced expansion, functional potential and cytolytic capacity of LCMV-specific CD8 T-cells (Fig. S5D–G) with minimal effects on LCMV-specific CD4 T-cells (Fig. S5H). Clearance of Arm infection relies solely on anti-viral CD8 T cells, thus inhibition of IFN-I antiviral effects coupled to abrogation of CD8 T-cell responses likely contributed to defective control of Arm infection.

To measure localization of naïve T-cells to T-cell zones in the spleen, CFSE-labeled naïve T-cells were adoptively transferred into Cl13-infected mice treated with isotype or anti-IFNAR1 antibodies. Naïve T-cells migrated to T-cell zones in anti-IFNAR treated mice similar to naïve controls 5 dpi. Comparatively, although T-cell zones were intact in isotype treated mice, naïve T-cells did not remain in these areas (Fig 4A&B) despite similar numbers of naïve CFSE labeled T-cells in the spleen. At 14 dpi, differences in naïve T-cell localization between anti-IFNAR1 and isotype control treated mice were maintained (Fig. 4B). Analysis of virus-specific T-cell function revealed that the numbers of GP33-specific IFN-γ^+ or IFN-γ^+TNF-α^+IL-2^+ multifunctional cytokine-producing cells (Fig. 4C) along with cytolytic potential (Fig. S6A) following anti-IFNAR1 treatment were comparable to isotype control treated mice while there was a significant decrease in IFN-γ^+TNF-α^+ GP33-specific CD8 T-cells (Fig. 4C). In contrast, GP61-specific IFN-γ^+ and multifunctional CD4 T-cells 9 dpi were elevated in anti-IFNAR1 compared to control treated mice (Fig. 4D). Despite elevated numbers and enhanced functional potential of virus specific CD4 T-cells, we observed similar levels of LCMV-specific IgG in the serum (Fig. S6B), demonstrating that IFN-I blockade enhances virus-specific CD4 T-cell responses while maintaining antiviral CD8 T-cell and antibody levels.

Because blockade of IFN-I signaling resulted in significantly elevated virus-specific CD4 T-cells responses, we asked whether CD4 T-cells were required for virus control following IFN-I blockade. Antibody depletion of CD4 T-cells had little effect on anti-IFNAR1-mediated reduction of viral titers on day 21 post-infection (Fig. 4E) however, by 40 and 50 dpi, CD4-depletion completely abrogated the anti-IFNAR1-mediated reduction in viral titers compared to CD4-sufficient, IFNAR1-treated mice (Fig. 4E&F). Anti-IFNAR1 treatment following CD4 depletion had no effect on controlling Cl13 replication in lung, kidney and

brain 75 dpi (Fig. 4G). These data demonstrate CD4 T-cells are required for enhanced control of persistent virus infection following IFN-I blockade.

We identify IFN-I signaling as essential for immune activation, up-regulation of negative immune regulators, lymphoid disorganization and virus persistence. IFN-I has pleiotropic effects on multiple cellular processes. Aside from antiviral effects (25), IFN-I signaling influences cell differentiation, proliferation and apoptosis (26). Further, multiple pro-inflammatory mediators are downstream of IFN-I signaling; thus IFN-I can regulate multiple physiological processes. Despite discovery of IFN-I over 50 years ago (27), its mechanisms of action with respect to immune modulation (25) or antiviral activity (28, 29) remain unsettled.

Chronic immune activation following HIV infection is documented and suppression of this hyper-activated state may alleviate pathologies associated with HIV infection (7). Disease following experimental SIV infection in rhesus macaques correlates with elevated IFN-I and inflammatory signatures (30, 31). In contrast, SIV infection in sooty mangabeys and African green monkeys, which develop modest pathology despite similar viral loads as macaques, correlate with reduced IFN-I and inflammatory signatures (32). Similar correlations with respect to reduced immune activation exist in HIV infected elite controllers, although whether reduced immune activation follows better control of virus infection is debatable (33, 34). Moreover, an elevated interferon signature is observed in HCV-infected patients despite limited control of virus replication and development of liver pathology (35, 36). Thus, the IFN-I signaling pathway may be a viable target to control persistent viral infections.

Supplementary Material

Refer to Web version on PubMed Central for supplementary material.

Acknowledgments

The authors thank D. Fremgen, C. Cubitt, N. Ngo and S. Rice for technical excellence. Data reported in the manuscript are tabulated in the main paper and in the supplementary materials. This research was supported by NIH grant AI09484 (MBAO), grants NCI CA43059 (RDS), U54AI057160 to the Midwest Regional Center of Excellence for Biodefense and Emerging Infectious Diseases Research (MRCE) (RDS and MBAO), grant AI077719 (JCT) and postdoctoral training grants AI007354 and American Heart fellowship 11POST7430106 (JT), HL007195 (CN) and NS041219 (BS).

REFERENCES

1. Brooks DG, et al. Nat Med. 2006 Nov.12:1301. [PubMed: 17041596]
2. Barber DL, et al. Nature. 2006 Feb 9.439:682. [PubMed: 16382236]
3. Yi JS, Cox MA, Zajac AJ. Immunology. 2010 Apr.129:474. [PubMed: 20201977]
4. Zajac AJ, et al. J Exp Med. 1998 Dec 21.188:2205. [PubMed: 9858507]
5. Appay V, Sauce D. The Journal of pathology. 2008 Jan.214:231. [PubMed: 18161758]
6. Chang JJ, Altfeld M. The Journal of infectious diseases. 2010 Oct 15.202(Suppl 2):S297. [PubMed: 20846036]
7. d'Ettorre G, Paiardini M, Ceccarelli G, Silvestri G, Vullo V. AIDS research and human retroviruses. 2011 Apr.27:355. [PubMed: 21309730]
8. Sevilla N, et al. J Exp Med. 2000 Nov 6.192:1249. [PubMed: 11067874]
9. Ahmed R, Salmi A, Butler LD, Chiller JM, Oldstone MB. J Exp Med. 1984 Aug 1.160:521. [PubMed: 6332167]
10. Salvato M, Borrow P, Shimomaye E, Oldstone MB. J Virol. 1991 Apr.65:1863. [PubMed: 1840619]

11. Evans CF, Borrow P, de la Torre JC, Oldstone MB. J Virol. 1994 Nov.68:7367. [PubMed: 7933120]
12. Sullivan BM, et al. Proc Natl Acad Sci U S A. 2011 Feb 15.108:2969. [PubMed: 21270335]
13. Bergthaler A, et al. Proc Natl Acad Sci U S A. 2010 Dec 14.107:21641. [PubMed: 21098292]
14. Scheu S, Dresing P, Locksley RM. Proc Natl Acad Sci U S A. 2008 Dec 23.105:20416. [PubMed: 19088190]
15. Macal M, et al. Cell host & microbe. 2012 Jun 14.11:617. [PubMed: 22704622]
16. Sheehan KC, et al. Journal of interferon & cytokine research : the official journal of the International Society for Interferon and Cytokine Research. 2006 Nov.26:804.
17. Sevilla N, McGavern DB, Teng C, Kunz S, Oldstone MB. J Clin Invest. 2004 Mar.113:737. [PubMed: 14991072]
18. Oldstone MB, Campbell KP. Virology. 2011 Mar 15.411:170. [PubMed: 21185048]
19. Muller S, et al. J Virol. 2002 Mar.76:2375. [PubMed: 11836415]
20. Berger DP, et al. Virology. 1999 Jul 20.260:136. [PubMed: 10405365]
21. Suresh M, et al. J Virol. 2002 Apr.76:3943. [PubMed: 11907234]
22. Zeng M, et al. J Clin Invest. 2011 Mar 1.121:998. [PubMed: 21393864]
23. Zeng M, et al. PLoS Pathog. 2012 Jan.8:e1002437. [PubMed: 22241988]
24. Hahm B, Trifilo MJ, Zuniga EI, Oldstone MB. Immunity. 2005 Feb.22:247. [PubMed: 15723812]
25. Stetson DB, Medzhitov R. Immunity. 2006 Sep.25:373. [PubMed: 16979569]
26. Platanias LC. Nat Rev Immunol. 2005 May.5:375. [PubMed: 15864272]
27. Isaacs A, Lindenmann J. Proc R Soc Lond B Biol Sci. 1957 Sep 12.147:258. [PubMed: 13465720]
28. Schoggins JW, Rice CM. Current opinion in virology. 2011 Dec.1:519. [PubMed: 22328912]
29. Schoggins JW, et al. Nature. 2011 Apr 28.472:481. [PubMed: 21478870]
30. Manches O, Bhardwaj N. J Clin Invest. 2009 Dec.119:3512. [PubMed: 19959871]
31. Jacquelin B, et al. J Clin Invest. 2009 Dec.119:3544. [PubMed: 19959873]
32. Bosinger SE, et al. J Clin Invest. 2009 Dec.119:3556. [PubMed: 19959874]
33. Deeks SG, Walker BD. Immunity. 2007 Sep.27:406. [PubMed: 17892849]
34. Saez-Cirion A, Pancino G, Sinet M, Venet A, Lambotte O. Trends in immunology. 2007 Dec. 28:532. [PubMed: 17981085]
35. Su AI, et al. Proc Natl Acad Sci U S A. 2002 Nov 26.99:15669. [PubMed: 12441396]
36. Guidotti LG, Chisari FV. Annual review of pathology. 2006; 1:23.
37. Borrow P, Evans CF, Oldstone MB. J Virol. 1995 Feb.69:1059. [PubMed: 7815484]

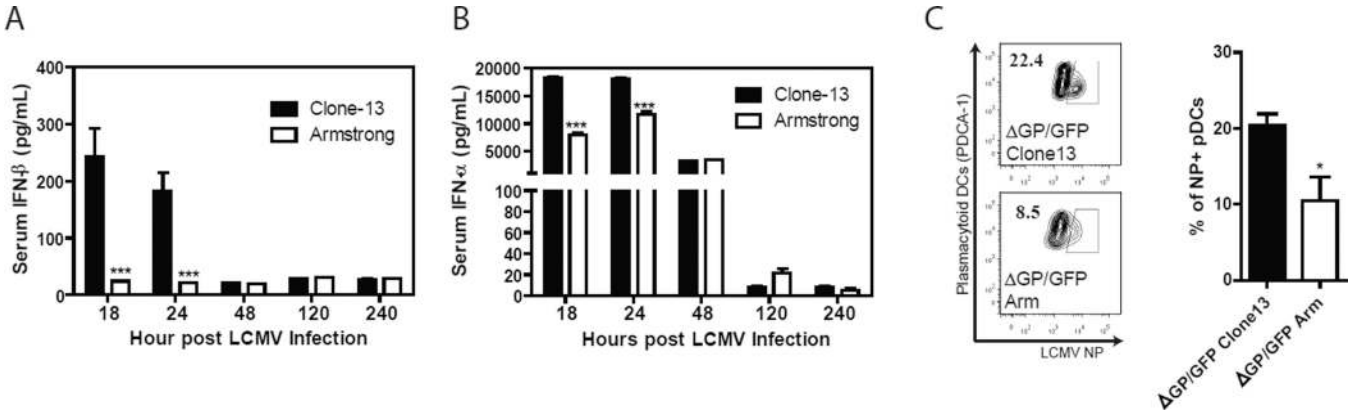

Figure 1.

IFN-I is elevated early following onset of persistent virus infection. Serum levels of interferon beta (A) and interferon alpha species (B) as measured by ELISA following initiation of persistent Cl13 or acute Arm infections in mice at 18, 24, 48, 120 and 240 hours post-infection in C57BL/6J mice. (C) pDCs are preferentially infected early following Cl13-infection. Percent of GFP positive pDCs infected with ΔGP clone-13 or Armstrong GFP viruses 24 hours post-infection. *, $p < 0.05$; **, $p < 0.01$; ***, $p < 0.005$. Results are representative of 2–3 independent experiments and represent the SEM from 3–5 mice/group.

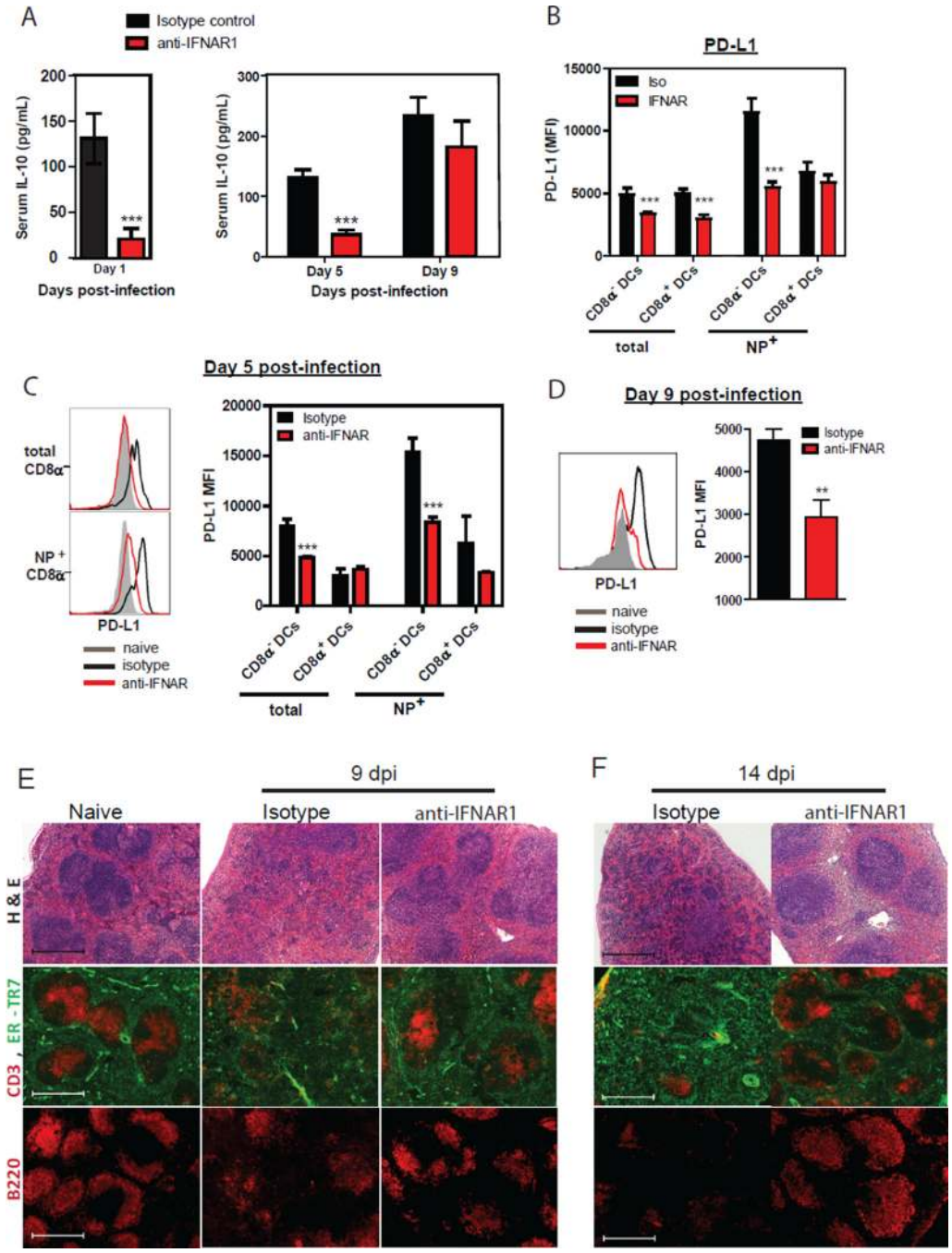

Figure 2.

IFN-I signaling is essential for the expression of the negative immune regulators IL-10 and PD-L1 and lymphoid tissue disorganization following persistent virus infection. Mice were treated with anti-IFNAR1 antibody 1 day prior to infection. (A) Serum levels of IL-10 as measured by ELISA on day 1, 5 and 9 post clone-13 infection in C57BL/6J mice treated with either isotype control or anti-IFNAR1 antibodies. (B) Mean fluorescent intensity (MFI) of PD-L1 expression as determined by flow cytometry on either LCMV viral antigen positive (VL-4^{+}) or viral antigen negative (VL-4^{-}) splenic DCs day 1 post clone-13 infection. (C) Representative histograms of PD-L1 expression as determined by flow cytometry on either infected or uninfected (shaded histograms) CD8α-negative DCs (left) or

compiled PD-L1 expression (right) at day 5 post-Cl13 infection. (D) Histogram of PD-L1 expression (left) and mean fluorescent intensity (right) as determined by flow cytometry on splenic CD8α-negative dendritic cells at day 9 post-Cl13 infection. Histopathological and immunofluorescent analysis of spleens day 9 (E) and day 14 (F) post Cl13 infection from naïve mice or mice infected with Cl13 and treated with isotype or anti-IFNAR1 antibodies as done above. Top row: H & E histopathological analysis. Middle row: staining for a stromal cell marker (ER-TR7, a marker for fibroblastic reticular cells) and T-cells (CD3). Bottom row: B cell staining (B220). Images were taken using a 5x objective . Scale bars = 500μm. *, $p < 0.05$; **, $p < 0.01$; ***, $p < 0.005$. Results are representative of 2 independent experiments and represent the SEM from 5 mice/group.

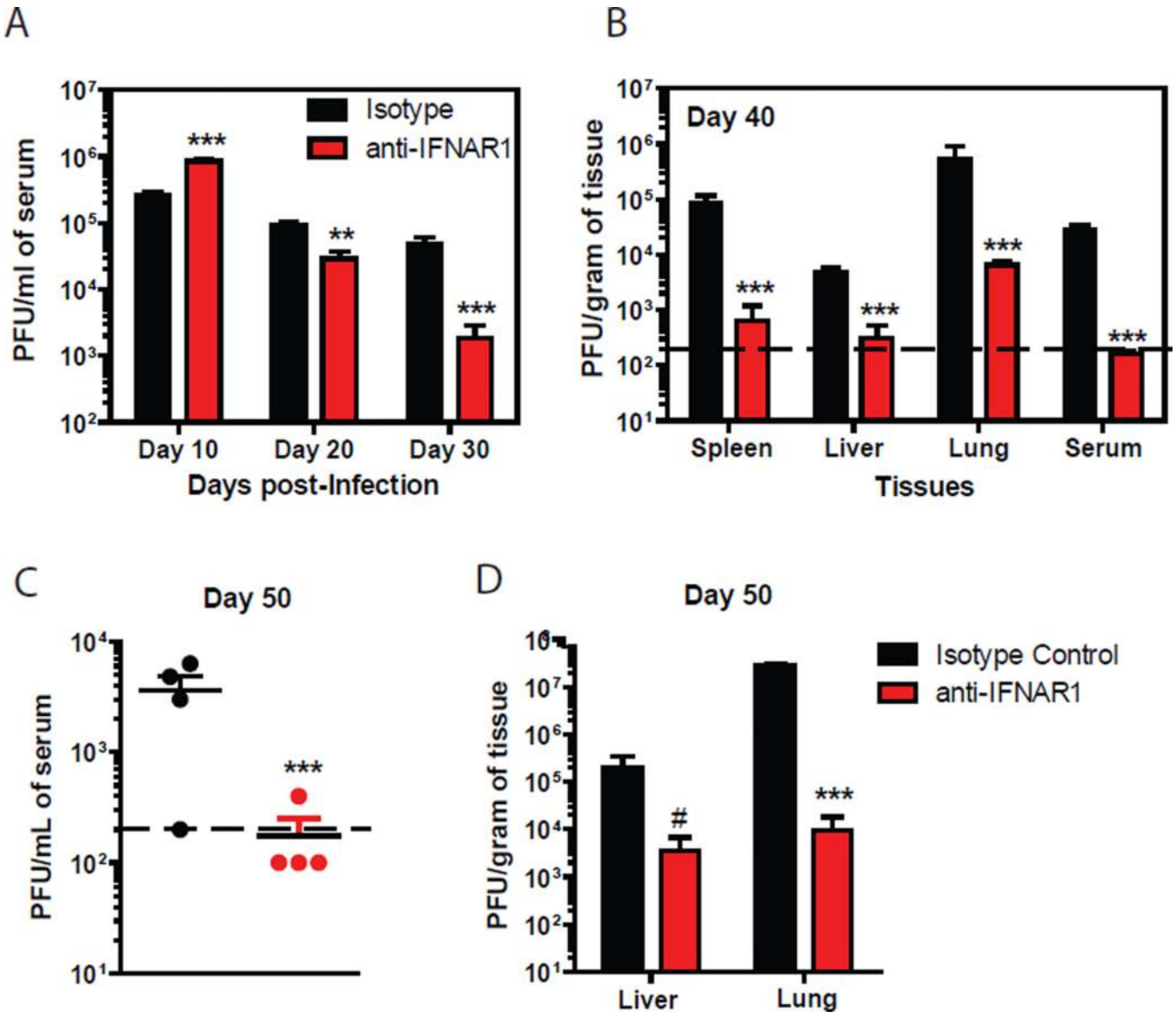

Figure 3.

IFN-I signaling blockade controls persistent virus infection. C57BL/6J mice were treated with either isotype control or IFNAR1 antibody 1 day prior to infection with Cl13 (A, B) or 10 days post-Cl13 infection (C–D). (A) Serum viral titers determined by plaque assay at the indicated times post-infection. (B) Viral titers in serum or indicated tissues at day 40 post infection. (C&D) Mice were infected with Cl13 and 10 days post-infection treated with 3 doses of anti-IFNAR1 antibody (500ug, Days 10 & 12 and 250ug day 14). The graph illustrates serum titers of mice 50 days post-infection in the serum (C), lung and liver (D). *, $p < 0.05$; **, $p < 0.01$; ***, $p < 0.005$ #, $p=0.07$. Results are representative of more than 5 independent experiments and represent the SEM from 5 mice per group.

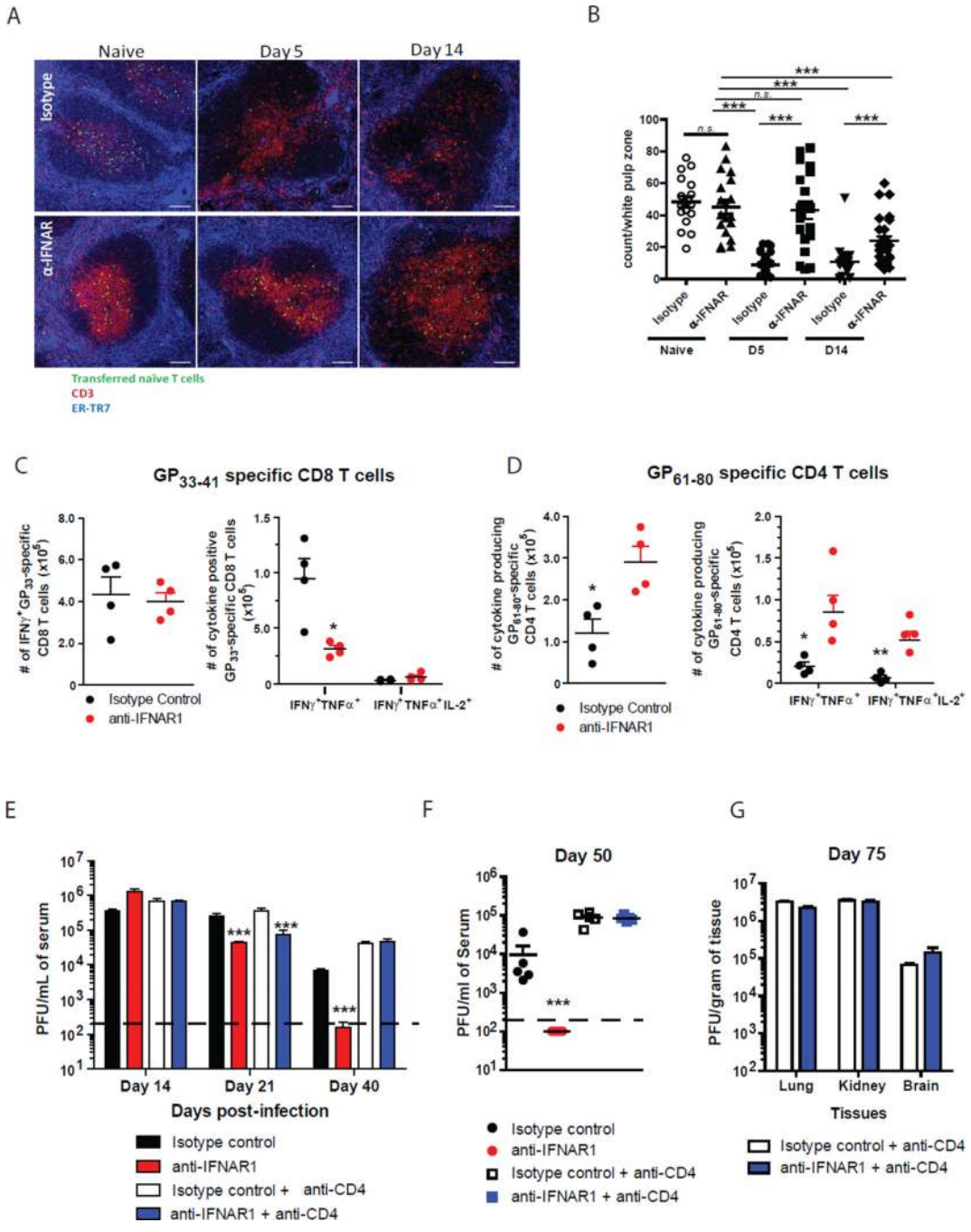

Figure 4.

Control of persistent virus by IFN-I blockade correlates with altered T-cell trafficking and requires CD4 T-cells. C57Bl/6J mice were treated with isotype control or IFNAR1 antibody prior to infection with CL13. (A) At 5 and 14 days post-infection, mice received adoptive transfers of CFSE-labeled naïve T-cells. 2 h after transfer, spleens were harvested to analyze homing and localization of naïve T-cells (green) to T-cell zones (CD3, red; fibroblastic reticular cells (ER-TR7), blue). Images were taken using a 20x objective. Scale bars = 100μm. (B) Quantitation of naïve T-cell localization. The number of transferred CFSE-labeled naïve T-cells was counted in ten random white pulp regions per spleen. (C) Total number of cytokine-producing $GP_{33–41}$ LCMV-specific CD8 T-cells in the spleen on day 9

post-infection. (D) Total number of cytokine-producing $GP_{61–80}$ LCMV-specific CD4 T-cells in the spleen on day 9 post-infection. (E–G) Mice treated with anti-CD4 and/or anti-IFNAR1 or control antibodies were infected with 2×10^6 PFU of Cl13 and viral titers were measured in the serum and tissues at the indicated times post-infection. Viral titers in the serum were quantified by plaque assay on days 14, 21 and 40 (E) and 50 (F) in the serum. (G) Depicts viral titers in the lung, kidney and brain in CD4-depleted mice treated with isotype or anti-IFNAR1 on day 75 post-infection. *, $p < 0.05$; **, $p < 0.01$; ***, $p < 0.005$. Results are representative of 2 independent experiments and represent SEM from 4–5 mice per group.